Reinvestigating 2,5-di(pyridin-2-yl)pyrazine ruthenium complexes

Schulz, M.; Hirschmann, J.; Draksharapu, A.; Singh Bindra, G.; Soman, S.; Paul, A.; Groarke, R.; T. Pryce, M.; Rau, S.; R. Browne, W.

Published in:
Dalton Transactions

DOI:
10.1039/c1dt10960j

Dalton Transactions

Dynamic Article Links

Cite this: *Dalton Trans.*, 2011, **40**, 10545

www.rsc.org/dalton

PAPER

Reinvestigating 2,5-di(pyridin-2-yl)pyrazine ruthenium complexes: selective deuteration and Raman spectroscopy as tools to probe ground and excited-state electronic structure in homo- and heterobimetallic complexes†

M. Schulz,[a] J. Hirschmann,[b] A. Draksharapu,[c] G. Singh Bindra,[a] S. Soman,[a] A. Paul,[a] R. Groarke,[a] M. T. Pryce,[a] S. Rau,[b] W. R. Browne*[c] and J. G. Vos*[a]

Received 22nd May 2011, Accepted 26th July 2011
DOI: 10.1039/c1dt10960j

The mono- (**1**) and dinuclear (**2**) ruthenium(II) bis(2,2′-bipyridine) complexes of 2,5-di(pyridin-2-yl)pyrazine (2,5-dpp), for which the UV/Vis absorption and emission as well as electrochemical properties have been described earlier, are reinvestigated here by resonance, surface enhanced and transient resonance Raman spectroscopy together with selective deuteration to determine the location of the lowest lying excited metal to ligand charge transfer (^{3}MLCT) states. The ground state absorption spectrum of both the mono- and dinuclear complexes are characterised by resonance Raman spectroscopy. The effect of deuteration on emission lifetimes together with the absence of characteristic bipy anion radical modes in the transient Raman spectra for both the mono- and dinuclear complexes bridged by the 2,5-dpp ligand confirms that the excited state is 2,5-dpp based; however DFT calculations and the effect of deuteration on emission lifetimes indicate that the bipy based MLCT states contribute to excited state deactivation. Resonance Raman and surface enhanced Raman spectroscopic (SERS) data for **1** and **2** are compared with that of the heterobimetallic complexes $[Ru(bipy)_2(2,5\text{-dpp})PdCl_2]^{2+}$ **3** and $[Ru(bipy)_2(2,5\text{-dpp})PtCl_2]^{2+}$ **4**. The SERS data for **1** indicates that a heterobimetallic Ru–Au complex forms *in situ* upon addition of **1** to a gold colloid.

Introduction

Over the last decades interest in dinuclear metal complexes, of the type M–BL–M′, where BL is a bridging ligand and M and M′ are polypyridyl complexes based on metals such as Ru, Os, Rh, Pt, Pd, Fe, Re, Cu and others has increased steadily.[1] The design of such compounds requires consideration of the nature and location of the lowest unoccupied molecular orbital (LUMO) especially, for example, with regard to controlling the direction of photoinduced electron transfer. Since the seminal studies of Creutz and Taube,[2] the pyrazine moiety has seen widespread use as a component of bridging ligands. The primary reasons for its use include the expectation that the LUMO in dinuclear complexes of this type will be based on the bridging ligand rather than the peripheral polypyridyl ligands. Examples of such ligands include the 2,3- and 2,5-di(pyridin-2-yl)pyrazine ligands, 2,3-dpp, and 2,5-dpp, respectively.[3,4] The Kaim and Keene groups have studied these classes of bridged complexes in detail by (spectro)electrochemical methods,[5–7] while the Balzani group has focused on the excited state properties of these compounds.[8–14] The former studies were mostly focused on the 2,5-dpp containing complexes, whereas the latter focused mainly on photophysical studies on multinuclear complexes based on the 2,3-dpp ligand; with some systems containing up to twenty-two metal centres.[15,16] As a consequence of the 2,5-dpp ligand being unsuitable for the design and preparation of extensive multinuclear arrays, the photophysical properties of compounds containing this bridging ligand have received relatively less attention. The recent surge in interest in heterobimetallic complexes for photocatalytic hydrogen production however has renewed interest in 2,5-dpp bridged systems.

Recently, Brewer and co-workers reported the photocatalytic properties of a 2,3-dpp based Ru(II)–Rh(III)–Ru(II) triad for the light driven splitting of water. They proposed that the catalytic centre in this photocatalyst most likely consists of the Rh(I) core in combination with a reduced 2,3-dpp bridging ligand.[17,18]

Ozawa and Sakai have reported that the 2,5-dpp bridged Ru(II)–Pt(II) dinuclear complex does not produce hydrogen.[19] The absence of activity for this latter complex is the subject of this contribution as the lack of photocatalytic activity of this and

[a]*School of Chemical Sciences, Dublin City University, Glasnevin, Dublin, 9, Ireland. E-mail: han.vos@dcu.ie; Tel: 00353-1-700-5307*
[b]*Institut für Anorganische Chemie I, Materialien und Katalyse, Universität Ulm, Albert-Einstein-Allee 11, 89081, Ulm, Germany*
[c]*Stratingh Insitute for Chemistry, Faculty of Mathematics and Natural Sciences, University of Groningen, Nijenborgh 4, 9747AG, Groningen, The Netherlands. E-mail: w.r.browne@rug.nl*

† Electronic supplementary information (ESI) available: Synthesis and analytical data, additional Raman spectra. See DOI: 10.1039/c1dt10960j

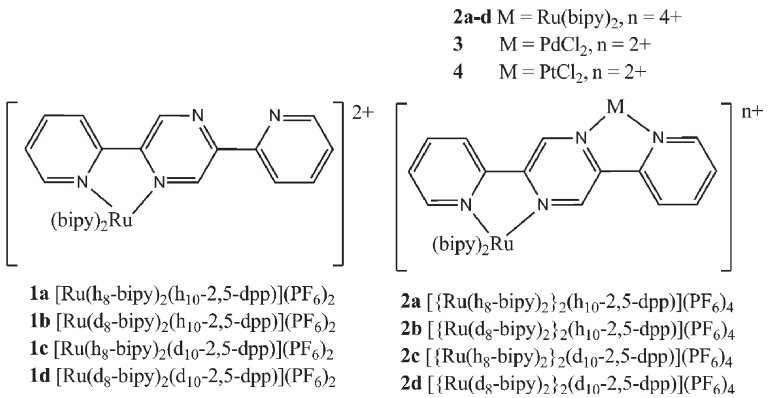

Fig. 1 Ruthenium polypyridyl complexes examined. Abbreviations: bipy = 2,2′-bipyridine; 2,5-dpp = 2,5-di(pyridin-2-yl)pyrazine.

related complexes may be overcome by changing the properties of the components present in such assemblies, in particular the nature of the peripheral ligands. This approach builds on recent studies by Rau and co-workers who proposed that for similar photocatalytic systems, the initial photophysical steps that follow photoexcitation are of substantial importance to the overall efficiency of the photocatalytic process.[20] For this reason detailed information is required regarding the photophysical properties of, in particular, 2,5-dpp based complexes.

Here, we report the characterisation of the complexes $[Ru(bipy)_2(2,5\text{-dpp})]^{2+}$ **1a–d**, $[(Ru(bipy)_2)_2(2,5\text{-dpp})]^{4+}$ **2a–d** and the heterobimetallic complexes $[Ru(bipy)_2(2,5\text{-dpp})PdCl_2]^{2+}$ **3** and $[Ru(bipy)_2(2,5\text{-dpp})PtCl_2]^{2+}$ **4** by UV/Vis absorption, emission and resonance Raman spectroscopy aided by selective deuteration of the ligands (Fig. 1). The goal of the study is two fold: firstly to determine the orbital parentage of visible and near-UV absorption bands and the localisation of the lowest ^{3}MLCT excited state and secondly to explore the potential of resonance Raman spectroscopy as a tool in mechanistic studies in photocatalytic dihydrogen production in heterobimetallic catalysts based on the 2,5-dpp bridging ligand such as $[Ru(bipy)_2dppPtCl_2]^{2+}$. In these studies deuteration is a key asset in simplifying the interpretation of ^{1}H-NMR spectra and in definitive assignment of vibrational modes observed by Raman spectroscopy. Furthermore it is an important tool in the determination of the degree of localisation of the lowest ^{3}MLCT states and the role of excited states based on each ligand in facilitating excited state deactivation.[21]

Results and discussion

Synthesis and characterisation

The complexes **1a–d** and **2a–d** were prepared by literature methods with either perprotio ligands, d_8-2,2′-bipyridine or d_{10}-2,5-di(pyridin-2-yl)pyrazine (Fig. 1). The heterobimetallic complexes $[Ru(bipy)_2(2,5\text{-dpp})PdCl_2]^{2+}$ (**3**) and $[Ru(bipy)_2(2,5\text{-dpp})PtCl_2]^{2+}$ (**4**) were prepared from **1a** and characterised by standard methods. The ^{1}H NMR spectra of the perprotio complexes have been assigned elsewhere[22] and hence only a brief discussion is made here. Deuteration of either the bipy or 2,5-dpp ligands facilitates assignment of the non-deuterated ligands. For example for **1b**, the absence of resonances of the bipy ligands allows for observation of ten resonances of 2,5-dpp (Fig. 2). The overlapping multiplets are assigned to the pyridyl moieties while the singlets are assigned to the pyrazine ring. The chemical shifts of the latter are influenced by the proximity of bipyridine ligands with the hydrogen *meta* to the

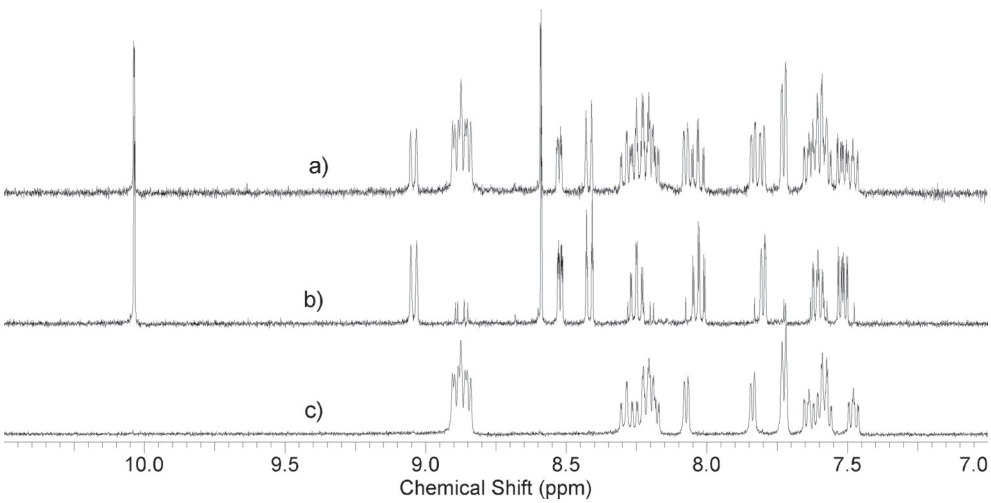

Fig. 2 Comparison of the ^{1}H NMR spectra of the perprotio and partially deuteriated mononuclear complexes: a) $[Ru(bipy)_2 2,5\text{-dpp}]^{2+}$ **1a**; b) $[Ru(bipy\text{-}d_8)_2 2,5\text{-dpp}]^{2+}$ **1b**; c) $[Ru(bipy)_2 dpp\text{-}d_{10}]^{2+}$ **1c**.

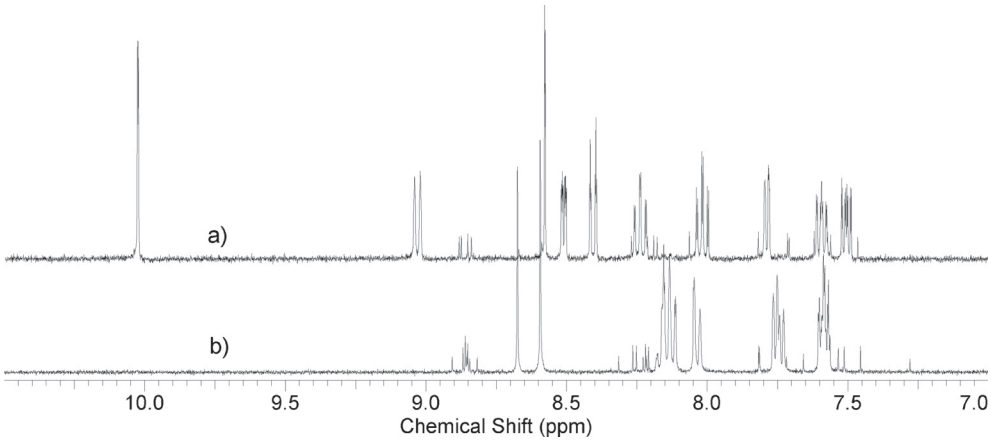

Fig. 3 ^{1}H NMR spectra of a) $[Ru(bipy\text{-}d_8)_2(2,5\text{-}dpp)]^{2+}$ **1b**; b) $[\{Ru(bipy\text{-}d_8)_2\}_2 2,5\text{-}dpp]^{4+}$ **2b**.

coordinated nitrogen being shifted downfield to *ca.* 10 ppm. For **2c**, the 2,5-dpp ligand is symmetric with both pyridines coordinated to $Ru(bipy)_2$- units. Furthermore the pyrazine hydrogens are now both shielded by proximity to bipy ligands and are at *ca.* 8.7 ppm. Ten resonances from the 2,5-dpp ligand are observed for **2b**, which confirms the presence of a mixture of ΛΛ/ΔΔ and ΔΛ diastereoisomers (Fig. 3).

Electronic properties

The UV/Vis absorption and emission spectra for **1a** and **2a** recorded in acetonitrile solution are shown in Fig. 4 and the data, together with emission lifetime data at 77 K in an alcohol glass, are summarized in Table 1. As expected, deuteration does not affect the absorption or emission spectra. All data for the perprotio complexes are in agreement with literature data.[6,11] The absorption spectra of **1a** and **2a** are similar with regard to the ππ* absorption of the bipy ligands at 285 nm and the ^{1}MLCT absorption band at 430 nm. The absorptions between 320 and 350 nm can be assigned to pyrazine based ππ* transitions (*vide infra*).[23] The band at 483 nm in **1a** is red-shifted to 585 nm in **2a** suggesting that it is a pyrazine based ^{1}MLCT transition. The emission lifetime data at room temperature in aerated acetonitrile are in agreement with lifetime data reported by Balzani and coworkers.[11]

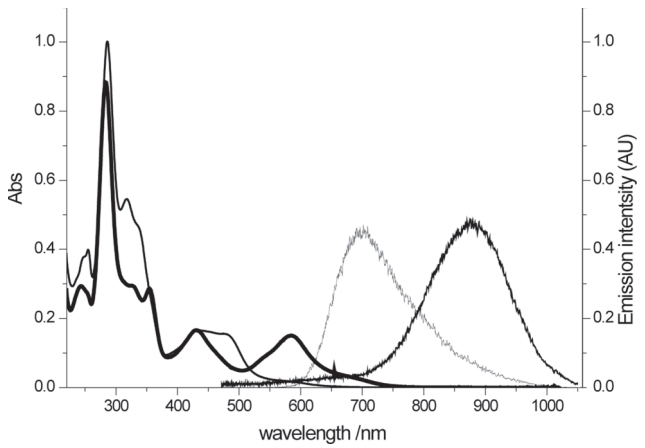

Fig. 4 Absorption and emission spectra for **1a** (thin lines) and **2a** (thick lines) in aerated acetonitrile at 298 K.

Table 1 Absorption and luminescence data for **1a–d** and **2a–d**

	Absorption[a]	Emission			
	293 K	293 K[a]		77 K[c]	
	λ_{max} [nm][b]	λ_{max} [nm]	τ/ns	λ_{max}/nm	t/μs
1a	483	695	266	638	3.6
1b	483	695	—	638	4.1
1c	483	695	—	638	4.5
1d	483	695	—	638	4.7
2a	585	875	114	764	2.0
2b	585	875	—	764	1.9
2c	585	875	—	764	3.4
2d	585	875	—	764	4.4

[a] Aerated acetonitrile solution. [b] Lowest energy maximum. [c] MeOH–EtOH (1 : 4 v/v) glass.

As discussed above selective ligand deuteration can provide an indication of localisation of the emitting state and the involvement of ^{3}MLCT states based on other ligands in the deactivation of the excited state. For example, for complexes of the type $[Ru(L^1)_2(L^2)]^{2+}$ where the ligand L^2 is deuterated, the lifetime of the emitting state will be longer only when the emitting state is based on the L^2 ligand, to a first approximation.[21,24] However, if coupling with higher excited states is significant then deuteration of the L^1 ligands would be expected to contribute to the increase in the emission lifetime also. For both **1a** and **2a** deuteration of either the bipy ligands and/or the 2,5-dpp ligand leads to an increase in emission lifetime at 77 K. However in both cases the effect of deuteration of the 2,5-dpp ligand is more pronounced indicating localisation of the emissive excited ^{3}MLCT state on the 2,5-dpp ligand, *i.e.* a $(\pi^*_{2,5\text{-}dpp} \leftarrow d_{t2g})^{3}$MLCT state (*vide infra*).

DFT of 1a and 2a

The calculated bond lengths and angles of **1a** and **2a** are in agreement with experimental data (Table 2).[19] However, the method overestimates the Ru–N bond lengths and the dihedral angle between the free pyridyl ring and the pyrazine moiety of **1a** (measured 32.5°; calculated 40.9°). In **2a** the coordination of two $Ru(bipy)_2$- units results in a near planar 2,5-dpp ligand.

The contributions of the selected moieties of the model complexes **1a** and **2a** to the individual molecular orbitals were

Table 2 Calculated and measure (from ref. 11) bond lengths (pm) and angles(°) for **1a** and **2a**

	Calc.		
Parameter	**1a**	**2a**	Exp.
Ru–N(bipy)	2.10	2.11	2.06
Ru–N(pyrazyl)	2.10	2.09	2.07
Ru–N(pyridyl)	2.09	2.10	2.03
N(bipy)–Ru–N(bipy)	78.4	78.2	78.0
N(pridyl)–Ru–N(pyrazyl)	78.6	78.4	81.8

calculated by a Mulliken population analysis (Fig. 5). The HOMO, HOMO−1 and HOMO−2 of **1a** and **2a** are metal-centred orbitals with minor contributions from the ligands. The main contributions to the LUMO are from the π* orbitals of the Ru(II) bound pyridine and pyrazine rings of 2,5-dpp. Both bipy ligands contribute to the LUMO of **1a**, however, for **2a** the contribution of the bipy ligands to the LUMO is negligibly small and it is localised on the entire 2,5-dpp ligand instead. The LUMO+1 has bipy π* character and is almost fully localised on the peripheral bipyridines with minor contributions from the bridging ligand and the metal centre. The LUMO+2 is a combination of bipyridine π* orbitals with minor contributions from metal-centred orbitals.

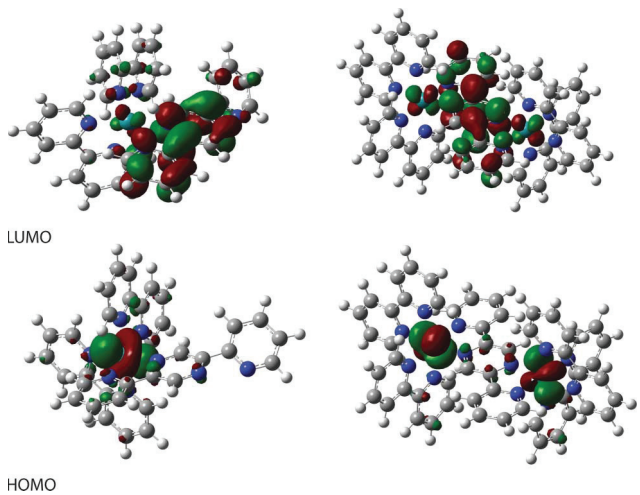

Fig. 5 HOMO and LUMO orbitals of (left) **1a** and (right) **2a**.

Resonance Raman (rR) spectroscopy of 1a–d and 2a–d

The UV/Vis absorption spectrum of **1a** shows three main absorptions at *ca.* 350, 430 and 480 nm. Resonance Raman (rR) spectroscopy can allow for the contribution of the bipy and 2,5-dpp ligands to these transitions to be determined. The relative contribution of the bipy and 2,5-dpp ligands to the rR spectra of **1a–d** can be assigned on the basis of isotopic shifts (Fig. 6). Deuteration of the bipy ligands did not affect the rR spectrum at 355 nm, however deuteration of the 2,5-dpp ligand results in a shift in all modes from 1605, 1592, 1568, 1513, 1492, 1472, 1443, 1432, 1377, 1320, 1296, 1242, 1185, 1036, 994 and 819 cm^{-1} for **1a** to 1561, 1532, 1495, 1453, 1395, 1314, 1289, 1234, 991, 968, 873 and 790 cm^{-1} for **1c**. This allows for the assignment of the transition at 355 nm as a 2,5-dpp based transition (presumably ππ* in origin, *vide infra*).

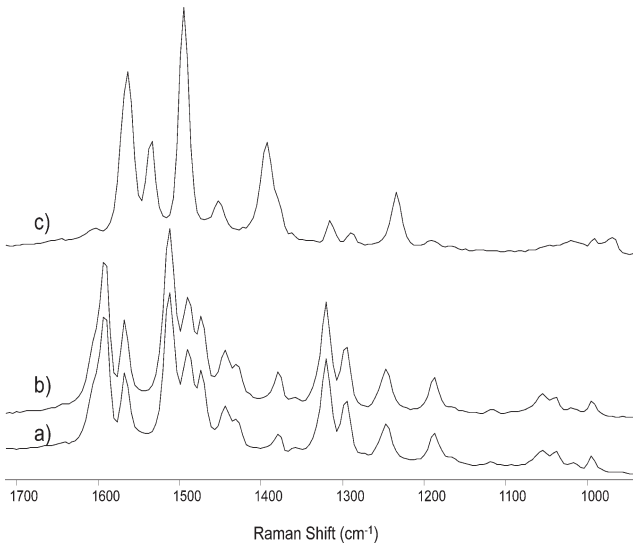

Fig. 6 rR spectra of (a) **1a**, (b) **1b** and (c) **1c** at λ_{exc} 355 nm in CH_3CN (solvent subtracted).

At λ_{exc} 450 nm, the rR spectra are again dominated by modes due to the 2,5-dpp ligand, however comparison of **1a** and **1b** showed that modes due to the bipy ligands are present in the spectra also, albeit at much lower intensity relative to the 2,5-dpp modes (Fig. 7). The bipy modes are typical of those observed upon excitation into a ^{1}MLCT ← GS transition.[25]

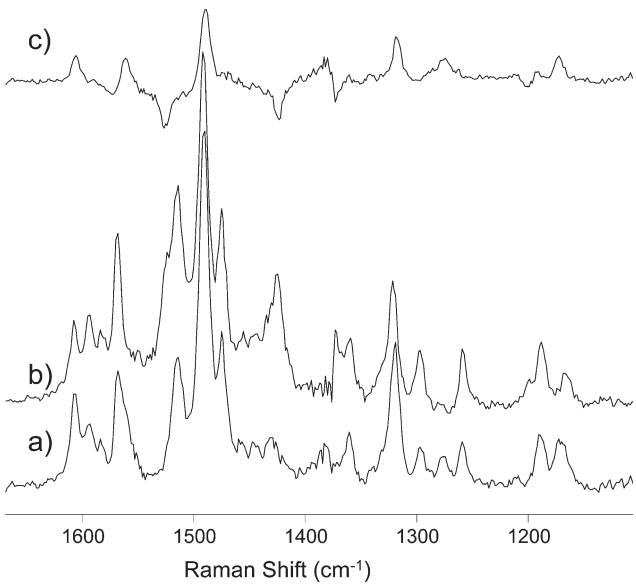

Fig. 7 rR spectra of (a) **1a**, (b) **1b** and (c) a scaled subtraction of the spectrum of **1b** from the spectrum of **1a** showing h_8-bipy modes as positive signals and d_8-bipy modes as negative signals. λ_{exc} 450 nm in CH_3CN (solvent subtracted).

The resonance Raman spectra of **2a–d** can be assigned on the basis of the isotopic shift, also. Deuteration of the bipy ligands did not affect the rR spectrum at 355 nm (Fig. 8), however, deuteration of the 2,5-dpp ligand results in a shift in all modes from 1596, 1482, 1466, 1319, 1114, 1069, 1049, 1018 and 827 cm^{-1} for **2a** to 1562, 1467, 1392, 1258, 1231, 1034, 988, 876 and 799 cm^{-1} for **2d**. This allows for the assignment of the transition at 355 nm as a 2,5-dpp

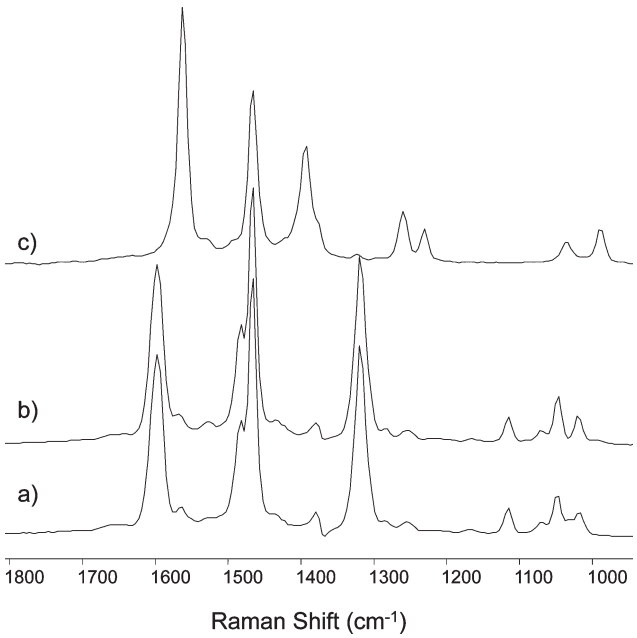

Fig. 8 Resonance Raman spectra of (a) **2a**, (b) **2b** and (c) **2d** λ_{exc} 355 nm in CH_3CN (solvent subtracted).

based transition (presumably ππ* in origin). The relative simplicity of the spectrum in comparison with that of the monomer reflects the increased symmetry in the dinuclear complex.

At λ_{exc} 450 nm the rR spectrum of **2a** (Fig. 9) is similar to that observed at 355 nm, however the modes at lower wavenumber are relatively less intense. Comparison of the spectra of **2a** and **2b** show that modes assignable to bipy ligands[25] are present albeit that they are relatively weak in comparison with those of the 2,5-dpp ligand. At 561 nm the rR spectra of **2a** and **2b** are identical and show no contribution from bipy modes. The correspondence of the rR spectrum of the dimer with its SERS spectrum (*vide infra*) is excellent with the exception of modes due to the bipy ligands which are absent in the rR spectra at 355 and 561 nm and weak in the spectrum at 450 nm. Notably in the rR spectra at 450 and 561 the modes in the 1300–1600 cm^{-1} region are enhanced most compared to the 355 nm rR and 785 nm SERS spectra reflecting the ^{1}MLCT ← GS character of the absorption bands in the visible region.

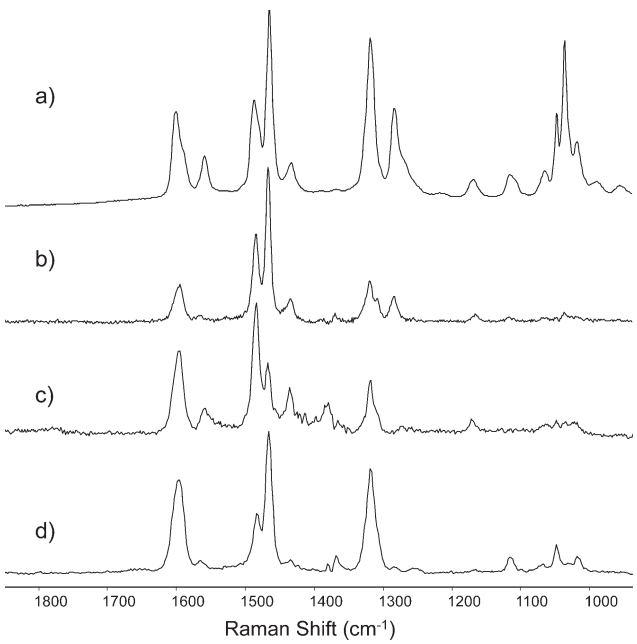

Fig. 9 Resonance Raman spectra of **2a** at λ_{exc} (a) 785 nm (SERS) (b) 561 nm, (c) 450 nm and (d) 355 nm in CH_3CN (solvent subtracted).

Transient resonance Raman (TR^2) spectroscopy

TR^2 spectroscopy using the single colour pump/probe method was employed at 355 nm to identify whether or not the bipy anion radical[25] (and hence a bipy based ^{3}MLCT state) was formed upon photoexcitation of the mono- and dinuclear complexes. Overall the TR^2 spectra obtained using pulsed excitation were identical to those obtained using continuous wave excitation at 355 nm as expected considering the strong ground state absorption of both **1a** and **2a** at 355 nm (Fig. 10). Importantly no evidence for the formation of a bipy anion radical was observed, *i.e.* the characteristic modes of bipy*$^-$ were absent. Confirmation that the pulse energy was sufficient to generate a significant excited state population was obtained from the power dependence. The intensity of the ground state modes decreased with increasing excitation pulse energy, relative to solvent bands (Fig. 11). This indicates that a significant depletion in the ground state absorption (and hence formation of the excited state) occurred at higher pulse energies. The absence of modes of the pyrazine anion radical (*i.e.* a pyrazine based ^{3}MLCT state) is not unexpected as excitation at 355 nm is almost certainly on the blue side of the excited state absorption (*i.e.* the ππ* transition of the pyrazine anion radical) since the ππ* absorption of the 2,5-dpp ligand is at 355 nm.[23]

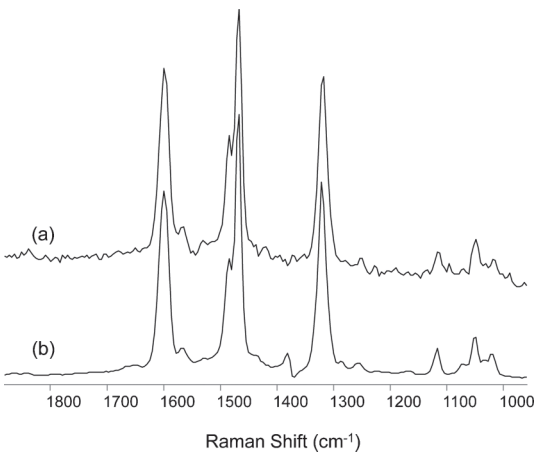

Fig. 10 (a) Transient (0.5 mJ per pulse) and (b) CW resonance Raman spectra of **2a** at λ_{exc} 355 nm in CH_3CN (solvent subtracted).

Surface enhanced Raman spectroscopy

Surface enhanced Raman spectra (SERS) were obtained by aggregation with 10 nm gold colloid. Again the availability of isotopologues allows for assignment of bipy and 2,5-dpp modes in the monomer and dimer. For **1a** modes assigned to the bipy ligands,[25] on the basis of comparison with the spectrum of **1b** (Fig. 12), are observed at 1603, 1560, 1488, 1314, 1272, 1170, 1166,

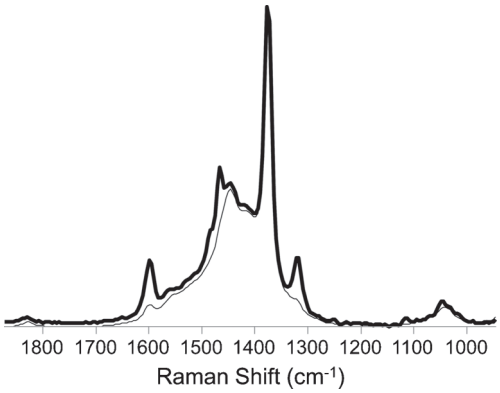

Fig. 11 TR^2 of **2a** at (thick line) low 0.5 mJ per pulse and (thin line) high power, 4 mJ per pulse) in CH_3CN showing a decrease in the intensity or the Raman modes of **2a** relative to solvent modes as the pulse power is increased.

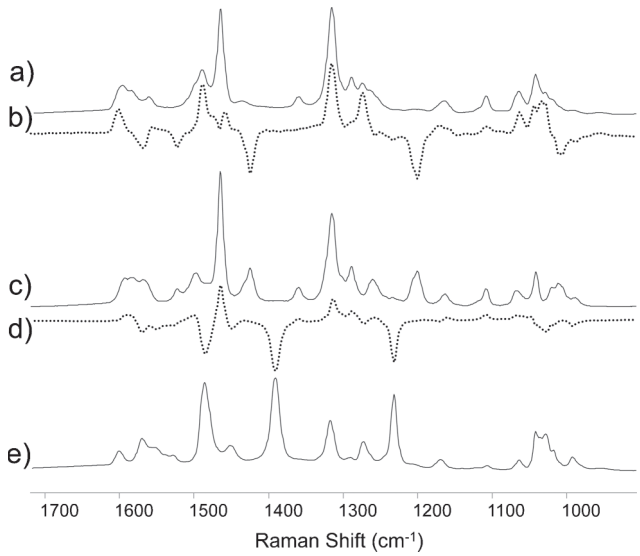

Fig. 12 SERS spectra of (a) **1a**, (b) subtraction of the spectrum of **1b** from that of **1a** showing h_8-bipy modes as positive signals and d_8-bipy modes as negative signals (c) **1b**, (d) subtraction of the spectrum of **1c** from that of **1a** showing h_{10}-2,5-dpp modes as positive signals and d_{10}-2,5-dpp modes as negative signals and (e) **1c**, λ_{ex} 785 nm on gold colloid self-aggregated.

1108, 1064, 1042 cm^{-1} (shifted to 1569, 1522, 1424, 1200, 1010 cm^{-1} for **1b**), and of the 2,5-dpp ligand at 1582, 1557, 1503 (shoulder), 1464, 1358, 1320, 1288, 1264 (shoulder) 1164, 1108 and 1068 cm^{-1} (shifted to 1569, 1551, 1483, 1448, 1392, 1296, 1274, 1232, 1030 and 991 cm^{-1} for **1c**). Overall the relative intensity of the bipy and dpp bands are similar.

The spectrum of **2a** is simpler than for **1a** as expected due to the increased symmetry of the dinuclear complex (Fig. 13). For **2a** modes assigned to the bipy ligands,[25] on the basis of comparison with the spectrum of **2b**, are observed at 1601, 1560, 1488, 1317, 1283, 1167, 1064 and 1034 and of the 2,5-dpp ligand at 1592(sh), 1465, 1432, 1320, 1118, 1048 and 1016 cm^{-1}. As for **1a** the relative intensity of the bipy and dpp bands in **2a** are similar.

Importantly the SERS spectrum of **1a** is substantially different not only in intensity pattern but also in band position compared with the rR spectra of **1a**. This is in contrast to **2a** (*vide supra*) and may indicate direct interaction (*e.g.*, coordination) with gold

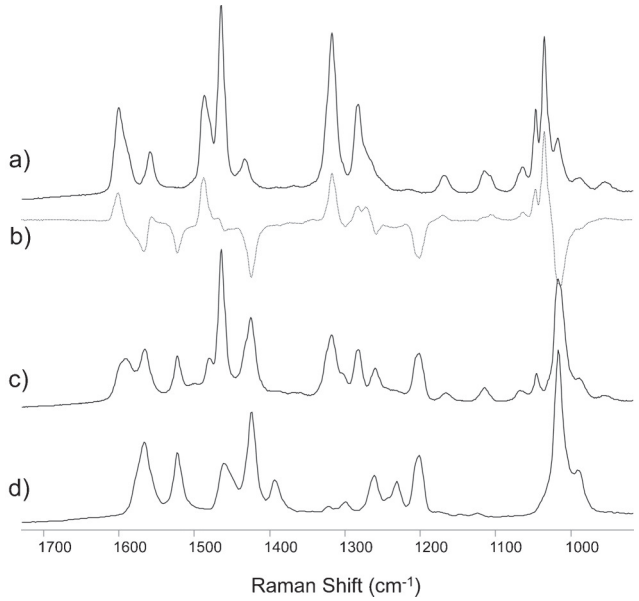

Fig. 13 SERS spectra of (a) **2a**, (b) subtraction of the spectrum of **2b** from that of **2a** showing h_8-bipy modes as positive signals and d_8-bipy modes as negative signals (c) **2b** and (c) **2d** λ_{exc} 785 nm on gold colloid, self-aggregated.

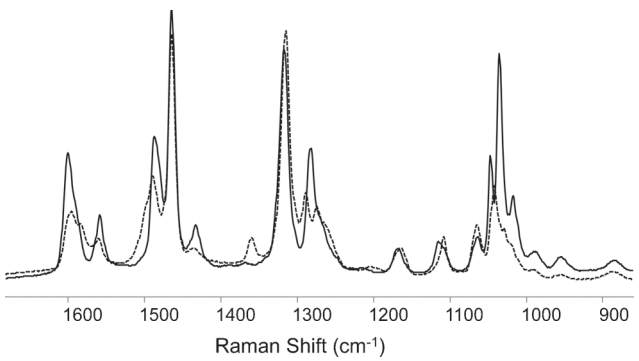

Fig. 14 SERS spectra of (a) **1a** (dashed line) and (b) **2a** (solid line), λ_{exc} 785 nm on gold colloid, self-aggregated.

under the conditions in which the SERS spectrum is obtained. Indeed the similarity of the SERS spectra of **1a** and **2a** supports this assignment (Fig. 14).

Resonance Raman of 3 and 4

The rR spectra of the mixed metal dinuclear complexes **3** and **4** at 355 (Fig. 15) and 532 nm are similar to those of **2a** and are dominated at all wavelengths by modes of the 2,5-dpp ligand. The UV/Vis absorption spectra of **3** and **4** (Fig. S2†) are broadly similar to that of **2a** and hence the same transitions are accessed at each wavelength for both **3**, **4** and **2a**. The spectra are very different to those of **1a**. As mentioned above, the similarity of the rR spectrum of **3** and **4** and the SERS spectrum of **1a** (Fig. 16) provides strong evidence that under the conditions in which the SERS spectrum of **1a** is obtained the free coordination site of the 2,5-dpp ligand is occupied by gold.

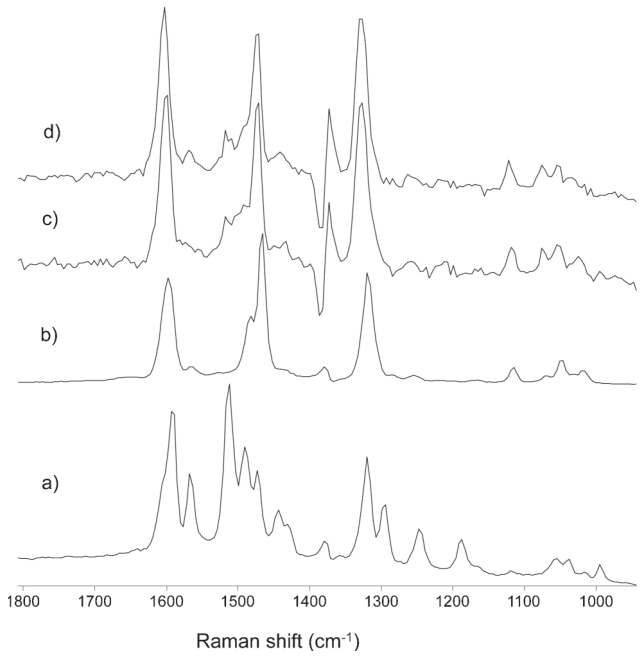

Fig. 15 rR spectra of (a) **1a** (b) **2a** (c) **3** and (d) **4** at λ_{exc} 355 nm in CH_3CN (solvent subtracted).

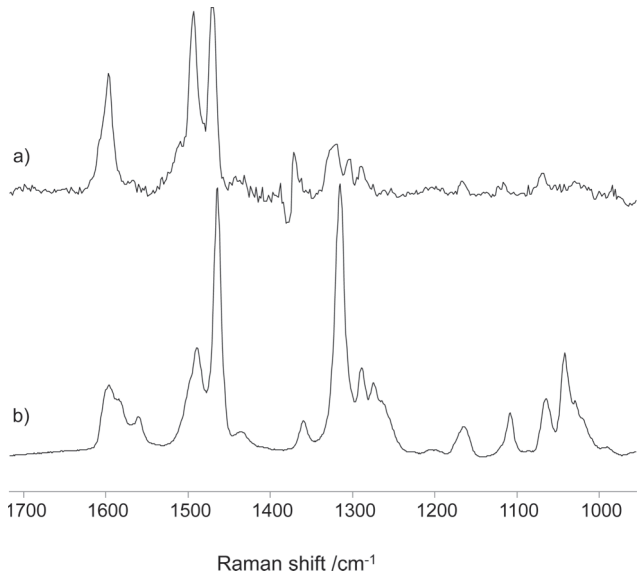

Fig. 16 (a) rR spectrum λ_{exc} 532 nm of **3** and (b) SERS spectrum of **1a** λ_{exc} 785 nm (on gold colloid, self-aggregated).

Conclusion

The emission and resonance Raman data reported in this contribution provide direct information concerning the nature of the electronic absorption bands in the near-UV and visible region and the localisation of the lowest lying excited state and the degree of involvement of higher lying excited states based on peripheral ligands in the excited state. The direct assignment is aided considerably by the availability of isotopologues. The lowest energy visible absorption bands and the absorption band at *ca.* 355 nm can be assigned as $\pi^*_{2,5\text{-dpp}} \leftarrow t_{2g}$ and $\pi\pi^*_{2,5\text{-dpp}}$ transitions, respectively and the lowest ^{3}MLCT excited state as a $^3(\pi^*_{2,5\text{-dpp}} \leftarrow t_{2g})$ state. This latter assignment is supported by comparison of the emission lifetimes of the **1a–d** and of **2a–d**, which show that the excited state deactivation is primarily affected by isotope substitution of the 2,5-dpp ligand with secondary contributions from deuteration of the bipy ligands and in the absence of characteristic modes of the bipy anion radical in the TR^2 spectra. Taken together this indicates that the stored 'photoexcited electron' will be on the ligand coordinated to the metal centre involved in catalysis in heterobimetallic complexes such as **3** and **4**. However it should not be assumed that the peripheral ligands are merely spectators as they are involved in excited state deactivation. This observation raises the prospect of tuning the photocatalytic activity of such complexes by substitution of the peripheral bipy ligands.

Under the conditions in which catalysis with complexes such as **3** and **4** is carried out a key mechanistic question arises as to the nature of the catalytically active species—specifically regarding whether the Pd/Pt remains coordinated to the 2,5-dpp ligand or instead forms nano-particulate species. The clear difference in the rR spectra of **1a** and **3/4** provides a key tool in answering these important questions as in the latter case the spectrum of **3** or **4** should revert to that of **1a** whereas if the complexes retain their hetereobimetallic structure then the rR spectrum should remain approximately unchanged even if the peripheral chlorido ligands on the Pd (or Pt) site are exchanged. It is expected that in fact some dissociation of the Pt/Pd will occur under reaction conditions. In this regard the time resolution achievable with resonance Raman spectroscopy (<1 min) should enable a detailed comparison of the rate and extent of dissociation with that of catalytic activity in terms of H_2 production.

Experimental

Reagents for synthesis were purchased as reagent grade and were used without further purification. 2,5-Di(pyridin-2-yl)pyrazine[26,27] was prepared according to the literature. The ligands, 2,2′-bipyridine (bipy) and 2,5-di(pyridin-2-yl)pyrazine[26,27] (2,5-dpp) were deuterated according to the methods reported earlier[28] at 200 °C in 1 M sodium deuteroxide in deuterium oxide.[24] The products were obtained with 97% deuterium incorporation. *bis*((d$_8$)-2,2′-Bipyridine)ruthenium(II) dichloride was prepared by literature methods.[11,5] Details of synthetic procedures and analytical data are available as ESI.†

NMR spectra were recorded on a Bruker Advance 400 spectrometer and referenced to the solvent signal. Elemental analysis was carried out on an Exador Analytical CE440 by the Microanalytical Department of the University College Dublin, treating deuterium as hydrogen. The fraction of hydrogen was calculated by multiplying the total number of hydrogen and deuterium atoms with the molecular weight of hydrogen and dividing by the actual molecular mass of the deuterated species. UV/Vis absorption spectra were recorded on Specord600 spectrophotometer (AnalytikJena) at 20 ± 1 °C in a 1 cm pathlength quartz cuvette. Acetonitrile for spectrophotometric measurements was purchased from Aldrich in spectrophotometric grade and used as received. Emission spectra and lifetimes (at 293 K) were obtained using an Andor technology iStar DH740 iccd with a shamrock163 spectrograph. A 300 mm^{-1} 300 nm blaze grating was used with calibration using a Hg/Ne lamp. The spectrograph was coupled to the sample holder by a 100 micron diameter fibre optic.

Sample excitation at 355 nm used the 3rd harmonic output of a spitlight400 Nd–YAG laser (Innolas) at 3 Hz with the flashlamps triggered externally by the digital delay generator of the iCCD. Emission spectra at 77 K were carried out in a liquid nitrogen filled glass cryostat using a mixture of ethanol and methanol (4 : 1 v/v) on a Perkin Elmer LS50B spectrofluorimeter for emission spectra and an Edinburgh Analytical Instruments TCSPC system with excitation with a pulsed LED at 360 nm for emission lifetime measurements. Raman spectra at 785 nm excitation were recorded using a Perkin Elmer Raman station. Gold colloid was prepared by standard procedures,[29] and aggregation occurred upon addition of dilute aqueous solutions of the complex to the colloid without the need for addition of other salts. Continuous wave Raman spectra at 355 nm (10 mW, Cobolt lasers), 450 nm (50 mW, Powertechnology), 532 nm (300 mW, Cobolt lasers) and 561 nm (100 mW, Cobolt lasers) were recorded using an 180° backscattering arrangement as described previously. Raman scattering was focused into a shamrock303i spectrograph and dispersed with either a 500 nm blaze 1800 mm^{-1} or 400 blaze 2400 mm^{-1} grating onto a iDus-BU2 CCD camera (Andor technology) cooled at −60 °C. Transient Raman spectra were recorded using the same system as for CW Raman studies except that a frequency tripled Nd–YAG laser (355 nm, 6 ns FWHM, with between 0.5 and 4 mJ per pulse, operating at 10 Hz, Innolas Spitlight 200). UV/Vis absorption spectra of samples before and after measurements were recorded to verify that photodecomposition did not occur during the acquisition of Raman spectra.

DFT calculations were performed using Gaussian 03.[30] The geometry of **1a** and **2a** was optimised in the gas phase at the B3LYP/LANL2DZ[31] level of theory using the GDIIS algorithm.[32] Tight convergence criteria were applied and a local minimum was confirmed by a frequency calculation (absence of imaginary frequencies). Orbital contributions were calculated in the gas phase at the B3LYP/LANL2DZ level using a Mulliken population analysis.

Acknowledgements

This research is supported by the EPA grant 2008-ET-MS-3-S2 and the SFI under Grants No. 07/SRC/B1160 and 08/RFP/CHE1349, an Ubbo Emmius Scholarship (AD) and the Netherland Organisation for Scientific Research through a VIDI grant (WRB).

Notes and references

1 P. Chen and T. J. Meyer, *Chem. Rev.*, 1998, **98**, 1439–1477; B. S. Brunschwig, C. Creutz and N. Sutin, *Chem. Soc. Rev.*, 2002, **31**, 168–184; K. D. Demadis, C. M. Hartshorn and T. J. Meyer, *Chem. Rev.*, 2001, **101**, 2655–2685; W. R. Browne, R. Hage and J. G. Vos, *Coord. Chem. Rev.*, 2006, **250**, 1653–1668.
2 C. Creutz and H. Taube, *J. Am. Chem. Soc.*, 1973, **95**, 1086–1094.
3 C. Hicks, J. Fan, I. Rutenberg and H. D. Gafney, *Coord. Chem. Rev.*, 1998, **171**, 71–84.
4 V. Balzani, A. Juris, M. Venturi, S. Campagna and S. Serroni, *Chem. Rev.*, 1996, **96**, 759–834.
5 S. Ernst, V. Kasack and W. Kaim, *Inorg. Chem.*, 1988, **27**, 1146–1148.
6 S. D. Ernst and W. Kaim, *Inorg. Chem.*, 1989, **28**, 1520–1528.
7 D. M. D'Alessandro and F. R. Keene, *New J. Chem.*, 2006, **30**, 228–237.
8 S. Campagna, G. Denti, S. Serroni, M. Ciano and V. Balzani, *Inorg. Chem.*, 1991, **30**, 3728–3732.
9 P. Ceroni, F. Paolucci, S. Roffia, S. Serroni, S. Campagna and A. J. Bard, *Inorg. Chem.*, 1998, **37**, 2829–2832.
10 G. Denti, S. Serroni, S. Campagna, V. Ricevuto and V. Balzani, *Inorg. Chim. Acta*, 1991, **182**, 127–129.
11 G. Denti, S. Campagna, L. Sabatino, S. Serroni, M. Ciano and V. Balzani, *Inorg. Chem.*, 1990, **29**, 4750–4758.
12 M. Marcaccio, F. Paolucci, C. Paradisi, S. Roffia, C. Fontanesi, L. J. Yellowlees, S. Serroni, S. Campagna, G. Denti and V. Balzani, *J. Am. Chem. Soc.*, 1999, **121**, 10081–10091.
13 M. Marcaccio, F. Paolucci, C. Paradisi, M. Carano, S. Roffia, C. Fontanesi, L. J. Yellowlees, S. Serroni, S. Campagna and V. Balzani, *J. Electroanal. Chem.*, 2002, **532**, 99–112.
14 M. Sommovigo, G. Denti, S. Serroni, S. Campagna, C. Mingazzini, C. Mariotti and A. Juris, *Inorg. Chem.*, 2001, **40**, 3318–3323.
15 S. Campagna, G. Denti, S. Serroni, A. Juris, M. Venturi, V. Ricevuto and V. Balzani, *Chem.–Eur. J.*, 1995, **1**, 211–221.
16 V. Balzani, S. Campagna, G. Denti, A. Juris, S. Serroni and M. Venturi, *Acc. Chem. Res.*, 1998, **31**, 26–34.
17 M. Elvington and K. J. Brewer, *Inorg. Chem.*, 2006, **45**, 5242–5244.
18 M. Elvington, J. Brown, S. M. Arachchige and K. J. Brewer, *J. Am. Chem. Soc.*, 2007, **129**, 10644–10645.
19 H. Ozawa and K. Sakai, *Chem. Commun.*, 2011, **47**, 2227–2242.
20 S. Tschierlei, M. Karnahl, M. Presselt, B. Dietzek, J. Guthmuller, L. Gonzalez, M. Schmitt, S. Rau and J. Popp, *Angew. Chem., Int. Ed.*, 2010, **49**, 3981–3984.
21 W. R. Browne and J. G. Vos, *Coord. Chem. Rev.*, 2001, **219–221**, 761–787.
22 M. B. Ferrari, G. G. Fava, G. Pelosi, G. Predieri, C. Vignali, G. Denti and S. Serroni, *Inorg. Chim. Acta*, 1998, **275–276**, 320–326.
23 W. R. Browne, N. M. O'Boyle, W. Henry, A. L. Guckian, S. Horn, T. Fett, C. M. O'Connor, M. Duati, L. De Cola, C. G. Coates, K. L. Ronayne, J. J. McGarvey and J. G. Vos, *J. Am. Chem. Soc.*, 2005, **127**, 1229–1241.
24 W. R. Browne, P. Passaniti, M. T. Gandolfi, R. Ballardini, W. Henry, A. Guckian, N. O'Boyle, J. J. McGarvey and J. G. Vos, *Inorg. Chim. Acta*, 2007, **360**, 1183–1190.
25 D. P. Strommen, P. K. Mallick, G. D. Danzer, R. S. Lumpkin and J. R. Kincaid, *J. Phys. Chem.*, 1990, **94**, 1357–1366.
26 F. Case and E. Koft, *J. Am. Chem. Soc.*, 1959, **81**, 905–906.
27 G. Clemo, T. Holmes and G. Leitch, *J. Chem. Soc.*, 1938, 753.
28 W. R. Browne, C. M. O'Connor, J. S. Killeen, A. L. Guckian, M. Burke, P. James, M. Burke and J. G. Vos, *Inorg. Chem.*, 2002, **41**, 4245–4251.
29 G. Frens, *Nature Phys. Sci.*, 1973, **241**, 20–22.
30 M. J. Frisch, G. W. Trucks, H. B. Schlegel, G. E. Scuseria, M. A. Robb, J. R. Cheeseman, J. A. Montgomery, Jr., T. Vreven, K. N. Kudin, J. C. Burant, J. M. Millam, S. S. Iyengar, J. Tomasi, V. Barone, B. Mennucci, M. Cossi, G. Scalmani, N. Rega, G. A. Petersson, H. Nakatsuji, M. Hada, M. Ehara, K. Toyota, R. Fukuda, J. Hasegawa, M. Ishida, T. Nakajima, Y. Honda, O. Kitao, H. Nakai, M. Klene, X. Li, J. E. Knox, H. P. Hratchian, J. B. Cross, V. Bakken, C. Adamo, J. Jaramillo, R. Gomperts, R. E. Stratmann, O. Yazyev, A. J. Austin, R. Cammi, C. Pomelli, J. Ochterski, P. Y. Ayala, K. Morokuma, G. A. Voth, P. Salvador, J. J. Dannenberg, V. G. Zakrzewski, S. Dapprich, A. D. Daniels, M. C. Strain, O. Farkas, D. K. Malick, A. D. Rabuck, K. Raghavachari, J. B. Foresman, J. V. Ortiz, Q. Cui, A. G. Baboul, S. Clifford, J. Cioslowski, B. B. Stefanov, G. Liu, A. Liashenko, P. Piskorz, I. Komaromi, R. L. Martin, D. J. Fox, T. Keith, M. A. Al-Laham, C. Y. Peng, A. Nanayakkara, M. Challacombe, P. M. W. Gill, B. G. Johnson, W. Chen, M. W. Wong, C. Gonzalez and J. A. Pople, *GAUSSIAN 03 (Revision D.01)*, Gaussian, Inc., Wallingford, CT, 2004.
31 A. D. Becke, *J. Chem. Phys.*, 1993, **98**, 5648–5652; C. T. Lee, W. T. Yang and R. G. Parr, *Phys. Rev. B*, 1988, **37**, 785–789; B. Miehlich, A. Savin, H. Stoll and H. Preuss, *Chem. Phys. Lett.*, 1989, **157**, 200–206; P. J. Hay and W. R. Wadt, *J. Chem. Phys.*, 1985, **82**, 270–283; P. J. Hay and W. R. Wadt, *J. Chem. Phys.*, 1985, **82**, 299–310; W. R. Wadt and P. J. Hay, *J. Chem. Phys.*, 1985, **82**, 284–298.
32 P. Csaszar and P. Pulay, *J. Mol. Struct.*, 1984, **114**, 31–34O. Farkas, Ph.D. Dissertation, Eötvös Loránd University and Hungarian Academy of Sciences, Budapest, 1995; O. Farkas and H. B. Schlegel, *J. Chem. Phys.*, 1999, **111**, 10806–10814.

